NJC

ROYAL SOCIETY OF CHEMISTRY

PAPER

View Article Online
View Journal | View Issue

Cite this: *New J. Chem.*, 2022, **46**, 10037

Characterization of lipase from *Candida rugosa* entrapped in alginate beads to enhance its thermal stability and recyclability†

Alice Vetrano, [a] Francesco Gabriele,[a] Raimondo Germani[b] and Nicoletta Spreti *[a]

Lipase from *Candida rugosa* has been immobilized in different formulations of calcium alginate beads, prepared by ionotropic gelation, which differ from each other in $CaCl_2$ concentration and hardening time, to investigate the effects of immobilization conditions on enzyme properties. Morphological studies on all hydrated beads, performed by SEM equipped with a Peltier plate, revealed a different internal compactness. Despite this, all types of beads had an immobilization yield of 100% measured with the Bradford method and about 94% evaluated from the residual activity of the preparation solutions; moreover, all entrapped biocatalysts catalyzed the complete hydrolysis of *p*-nitrophenyl acetate, even after one month of storage in distilled water at 4 °C. When the internal microstructure of the beads was more compact, the rate of hydrolysis of the most hydrophobic *p*-nitrophenyl dodecanoate was halved, probably due to mass transfer limiting effects. The immobilized lipase had better resistance to temperature inactivation than the free form: enzyme residual activity at 50 °C after a week were approximately 70% and 20% for the immobilized and free forms respectively. An excellent recyclability in water at 25 °C of entrapped enzyme was also found, having residual activity greater than 80% at the tenth reaction cycle. The best bead formulation was then used for the resolution of (*R*)-1-phenylethanol in aqueous solution starting from racemic (*R*,*S*)-1-phenylethyl acetate. The enantioselectivity found (E = 10) was slightly higher but did not differ significantly from that of free lipase towards the same substrate (E = 4).

Received 8th March 2022,
Accepted 3rd May 2022

DOI: 10.1039/d2nj01160c

rsc.li/njc

1. Introduction

The employment of enzymes as biocatalysts has emerged as an important tool in many industrial processes, such as the synthesis of active pharmaceuticals, detergents, food ingredients and fine chemicals.[1] However, although bioconversions are more environmentally friendly and more sustainable, some disadvantages limit the application of enzymes both in academic research and mainly in industry. These can be ascribed to the lack of operational stability and to the difficult recovery and reuse of biocatalysts, especially for their application in industrial processes, where multiple high yield cycles are required. Many technological implementations offer the possibility to overcome these drawbacks, such as reaction medium or protein and substrate engineering.[1] Immobilization techniques have also proven to be a very powerful tool for implementing enzyme properties.[2] In fact, immobilization, in addition to allowing easier recovery and reuse of the enzyme reducing operating costs, can improve other enzyme features, such as its stability in many reaction media, activity, selectivity, specificity, and resistance to temperature, chemicals and inhibitors.[3–5] The modification of enzyme properties due to its immobilization can sometimes be associated with changes in its structure in a more active form. Many other causes must also be considered, such as an increase in rigidity of the enzyme structure that avoids distortions, a protective effect of the support under harsh conditions, a decrease in substrate and/or product inhibition or the creation of their partition towards or away from the enzymatic environment.[3] Furthermore, in addition to the enzyme, the performance of an immobilized biocatalyst strongly depends both on the support materials (classic inorganic or organic supports and new materials with desired properties) and on the method of immobilization.[6–9] Several approaches have been investigated to improve enzyme performances, such as binding

[a] *Department of Physical and Chemical Sciences, University of L'Aquila, Via Vetoio – Coppito, I-67100 L'Aquila, Italy. E-mail: nicoletta.spreti@univaq.it*
[b] *CEMIN, Centre of Excellence on Nanostructured Innovative Materials, Department of Chemistry, Biology and Biotechnology, University of Perugia, Via Elce di Sotto 8, I-06123 Perugia, Italy*

† Electronic supplementary information (ESI) available. See DOI: https://doi.org/10.1039/d2nj01160c

(physical, ionic or covalent) to a support, cross-linking, which involves the formation of covalently linked protein-protein aggregates, or entrapment, in which the enzyme is physically confined within a three-dimensional polymeric network.[10–12] Each of them can affect enzyme properties and a universal method for enzyme immobilization still does not exist. Therefore, the appropriate choice of the best immobilization process must be made to obtain good catalytic activity, stability and reusability of the enzymes.[13]

Lipases (triacylglycerol ester hydrolase, E.C. 3.1.1.3) are ubiquitous enzymes widely employed to catalyze a wide range of enantio- and regioselective reactions such as hydrolysis, esterification, transesterification, aminolysis and ammoniolysis.[14–18] Unlike the usual esterases, lipases are able to hydrolyze long-chain acyl glycerols and contain an amphiphilic peptide lid domain covering the active site of the enzyme, which, in the presence of a hydrophobic interface, undergoes a conformational rearrangement allowing the enzyme to switch to the active state, a phenomenon known as interfacial activation.[19]

Lipase from *Candida rugosa* (CRL), whose structural features, mechanism of action and catalytic versatility are well known, exists as several isoenzymes, with a high structural homology, but different carbohydrate content, isoelectric point and substrate specificity.[20–23] CRL is one of the most used enzymes for biotransformations, but the use of the free form is not convenient, as it is deactivated when exposed to temperatures higher than 50 °C for a long time[24] and, above all, the enzyme is not recyclable and its separation from the final products requires many time-consuming steps. For these reasons, several methods have been reported to improve enzyme stability and recyclability: physical adsorption on solid supports,[25–29] cross-linking,[30–32] covalent binding[33–35] and encapsulation on a solid matrix.[36–39] Adsorption is the simplest and cheapest method, but the leaching of the enzyme from the support is a significant disadvantage for practical uses, compromising its reusability. Cross-linked enzyme aggregates, employing bifunctional reagents, can be either used as carrier-free macroparticles or immobilized on different supports[30,31] or they can be trapped in alginate beads.[32] In these cases, the operational stability and reusability of the biocatalyst have been improved and the immobilization protocol can be decisive due to the variety of enzyme structural conformations. Covalent binding to a support generally prevents enzyme leaching from the surface, but this method could have the disadvantage of a possible irreversible deactivation. Reusability, storage stability and tolerance to organic solvents were improved when CRL, chemically modified with a monomer of the metal–organic frameworks was used to the "*in situ*" synthesis of immobilized CRL composite,[33] as well as better lipase activity was achieved as a result of irreversible enzyme immobilization onto a ternary alginate/nanocellulose/montmorillonite composite.[34] The covalent immobilization of CRL onto magnetic beads offered important advantages in terms of enzyme reusability, thanks to the magnetically easy recovery of the biocatalyst from the reaction media, and can be applied for synthetic purpose,[35] for food applications,[40,41] and for biodiesel production.[42,43] Moreover, CRL, encapsulated in silica sol gels in the presence of magnetic sporopollenin/Fe_3O_4 nanoparticles,[36,37] β-cyclodextrin-grafted[38] and in the presence of *N*-methylglucamine based calix[4]arene magnetic nanoparticles[39] exhibited high thermal stability, reusability and excellent enantioselective capability.

Naturally-derived polymers turn out to be more advantageous in the entrapment of biomolecules than synthetic ones thanks to their intrinsic properties such as biocompatibility, non-toxicity, biodegradability and renewability that make them very attractive supports in many applications in biomedical, pharmaceutical and food sectors.[44] Among them, alginate, an anionic polysaccharide derived from brown algae consisting of β-D-mannuronate (*M*) and α-L-guluronate (*G*) as monomeric units, is by far the most widely used polymer for immobilization and microencapsulation technologies, thanks to its ability to easily form the desired three-dimensional structures in an aqueous environment by coordinating divalent cations.[45] Many alginate-based supports have been developed for enzyme immobilization and for the enhancement of enzyme properties, in terms of operational stability and reusability, together with their biotechnological applications, have recently been reviewed.[44] CRL was also entrapped in Ca-alginate beads and, thanks to the strong affinity of the polysaccharide for the enzyme, its thermal stability was improved as the energy barrier of the first deactivation step was higher than that of the free enzyme.[24] Nevertheless, the main problem was the CRL leaching from the beads,[46] that can be partially overcome by covering their surface with chitosan or silicate.[47] Esterification reactions were successfully performed in aqueous media using biphasic alginate beads, consisting of a solid matrix of calcium alginate and hexadecane,[48] or in organic solvents when CRL was immobilized in polyvinyl alcohol (PVA), alginate and boric acid beads.[49] In the latter case, the biocatalyst was more compatible with both water and organic media, since a certain amount of water molecules was also allowed in dehydrating solvents. The immobilization of CRL in magnetic alginate beads made possible to easily collect and reuse the biocatalyst for 6 cycles, but its activity was lower with respect to the enzyme entrapped in alginate beads.[50]

In this paper, CRL was immobilized within six different formulations of calcium-alginate beads. The operating conditions, such as the concentration of $CaCl_2$ and the residence time in the hardening solution, have been taken into account to evaluate their effect on: (i) loading efficiency; (ii) biocatalytic hydrolysis toward two substrates with different hydrophobicity *p*-nitrophenyl acetate (*p*-NPA) and *p*-nitrophenyl dodecanoate (*p*-NPD); (iii) recyclability and thermostability of the immobilized biocatalyst, decisive properties for industrial applications, and (iv) internal structure. Finally, the best formulation was chosen to perform the kinetic resolution of the racemic ester (*R*,*S*)-1-phenylethyl acetate.

2. Experimental section

2.1 Chemicals

Alginic acid sodium salt from brown algae (low viscosity), lipase from *Candida rugosa* (CRL, type VII, >1000 U mg^{-1} solid), *p*-nitrophenyl acetate (*p*-NPA), *p*-nitrophenyl dodecanoate (*p*-NPD),

racemic (*R*,*S*)-1-phenylethanol and (*R*)-(+)-1-phenylethanol were purchased from Sigma Aldrich. Racemic (*R*,*S*)-1-phenylethyl acetate was obtained from Merck. Coomassie Brilliant Blue G-250 dye was supplied by Bio-Rad. Enzyme and substrate were used with no further purification. All other chemicals used were of analytical grade.

2.2 Entrapment of CRL in calcium alginate beads

After an optimization of the shape and resistance to magnetic stirring, the best six bead formulations were reported in Table 1; they differed from each other in the concentration of the calcium chloride solution and in the residence time in the solution itself. CRL (2 mg ml^{-1}) was added in a 5% (w/v) alginate aqueous solution and the mixture was stirred thoroughly to ensure complete mixing. Two ml of the resulting solution were withdrawn with a syringe with a 23G needle (inner diameter 600 μm) and dropped at a distance of about 2 cm into a 2% or 5% calcium chloride solution, maintained under mechanical stirring at 50 rpm, obtaining about 120 beads with a total weight of 1.2 ÷ 1.4 g. After the formation of the beads, they were left in the calcium chloride solution for a time ranging from 10 min to 1 h, to increase their mechanical strength. Finally, the beads were filtered under vacuum and rinsed with distilled water to remove the excess of calcium chloride solution.

2.3 Immobilization efficiency

Loading efficiency was determined by checking the amount of CRL in both the bead preparation and washing solutions using the Bradford method.[51] A calibration curve was obtained by measuring the absorbance of solutions containing from 0 to 0.3 mg ml^{-1}, prepared from a stock solution with a CRL concentration of 2 mg ml^{-1}, at λ = 595 nm. The resulting calibration curve had a R^2 correlation coefficient of 0.99. The loss of enzyme from beads over time was assessed similarly. In addition, the activity of the solution used to prepare the beads was also measured and subtracted from that of the free enzyme in order to determine the immobilized activity and therefore the immobilization yield (%):[52]

$$\text{Yield } (\%) = \frac{\text{Immobilized activity}}{\text{Starting activity}} \times 100 \qquad (1)$$

We have taken as starting activity that of the free enzyme since the entrapment process is very fast. Moreover, the immobilization efficiency, that is the percentage of the immobilized activity that remains after the entrapment (observed activity), was calculated as:[2]

$$\text{Efficiency } (\%) = \frac{\text{Observed activity}}{\text{Immobilized activity}} \times 100 \qquad (2)$$

Table 1 Composition of alginate bead formulations[a]

	$CaCl_2$, % (w/v)	Residence time, min
Beads 1	2	10
Beads 2	5	10
Beads 3	2	30
Beads 4	5	30
Beads 5	2	60
Beads 6	5	60

[a] Sodium alginate solution 5% (w/v) and CRL 2 mg ml^{-1}.

2.4 CRL activity assay

Hydrolytic activity of lipase was determined by spectrophotometric measurements, by using Shimadzu UV-160A instrument, following the hydrolysis reaction of *p*-nitrophenyl acetate (*p*-NPA); the procedure was adapted from literature to this case of study.[53] Beads (1.2 ÷ 1.4 g – 4 mg CRL) were placed in a reaction vessel containing 9 ml of distilled water; then, 1 ml of substrate stock solution (100 mM *p*-NPA in CH_3CN) was added to the vessel in order to start the reaction. The reaction was carried out at room temperature under mild stirring and monitored at different times, taking 20 μl from the reaction solution, placing them in the 1 ml cuvette, where 0.98 ml of distilled water were already present. Spectrophotometric measurements were performed at λ = 348 nm, which corresponds to the isosbestic point of the equilibrium between *p*-nitrophenol/*p*-nitrophenoxide (*p*-NP), with a molar extinction coefficient as 5400 M^{-1} cm^{-1}. Once the reaction was completed, the beads were filtered under vacuum, washed, placed in a container with distilled water and stored at 4 °C.

Activity of encapsulated lipase was also determined with a more hydrophobic substrate, *p*-nitrophenyl dodecanoate (*p*-NPD), dissolved in CH_3CN; 1 ml of a 100 mM stock solution was placed in the reaction vessel containing 9 ml of *tert*-butyl alcohol as a solvent and the beads containing the enzyme (1.2 ÷ 1.4 g – 4 mg CRL). The reaction was monitored at different times following the appearance of *p*-NP at 348 nm.

2.5 CRL reusability

The stability of the encapsulated CRL and its reuse were tested under the same conditions described in the previous section. After each cycle, the biocatalyst was filtered, washed with water several times to remove any product adsorbed on the beads and reintroduced into a fresh reaction medium. The substrate hydrolysis reaction was assayed at appropriate time intervals up until its complete conversion to product.

2.6 Thermostability

Thermal stability of free and immobilized CRL was studied. Both forms of the enzyme were incubated in distilled water at 25 and 50 °C for various periods, from 8 h up to one week. The *p*-NPA hydrolysis reaction was conducted at the incubation temperatures for 30 min in pure water to determine both the initial and the remaining activity.

2.7 Kinetic resolution of racemic 1-phenylethyl acetate

Hydrolysis reaction of (*R*,*S*)-1-phenylethyl acetate was performed by placing 1 ml from a stock solution (100 mM in CH_3CN) into the reaction vessel containing 9 ml of water and

1.2 ÷ 1.4 g of beads. At different times, the beads were separated by filtration under vacuum, the aqueous phase was extracted with ethyl ether and, after the solvent was removed, isopropanol was added to the flask. The conversion, as well as the enantiomeric excess value (*ee*%) of the reagents and products were determined by HPLC analysis with an Agilent – 1220 Infinity II instruments equipped with a chiral column (Lux Cellulose-1) using 99 : 1 hexane/isopropanol as eluent at a flow rate of 0.6 ml min^{-1}. The retention times were 3.6, 3.9, 14.7, 18.5 min for (*R*)-1-phenylethylacetate, (*S*)-1-phenylethylacetate, (*R*)-1-phenylethanol, and (*S*)-1-phenylethanol, respectively. The enantiomeric excess of the substrate (ee_s) and product (ee_p), conversion (*c*) and enantioselectivity (*E*), the latter determined with the actual values of *c* and *ee*, were calculated by applying the following equations:[54]

$$ee_s(\%) = \frac{|R-S|}{|R+S|} \times 100 \quad (3)$$

$$ee_p(\%) = \frac{|R-S|}{|R+S|} \times 100 \quad (4)$$

$$c\ (\%) = \frac{ee_s}{ee_s + ee_p} \times 100 \quad (5)$$

$$E = \frac{\ln[(1-c)(1-ee_s)]}{\ln[(1-c)(1+ee_s)]} \quad (6)$$

where *R* was values of peak areas for (*R*)-1-phenylethanol and its ester, whereas *S* was values of peak areas for (*S*)-1-phenylethanol and its ester.

2.8 Morphological characterization

The shape and size of the beads were analyzed using Leica S8APO stereoscopic microscope with EC3 camera connected to a computer. The diameters distribution of the beads was evaluated by using the variance coefficient (CV), which indicates the deviation of each diameter (D_n) from the average value (D_m), and was determined as follows:

$$CV = \frac{1}{D_m}\sqrt{\frac{\sum_{n=1}^{n}(D_n - D_m)^2}{n-1}} \times 100 \quad (7)$$

Generally, with a CV less than 5%, 20–30 beads are sufficient for measurement of sphericity indicator because they are generally uniform in size.[55]

Sphericity factor (SF), indicating the roundness of the beads, was determined by using the following equation:[55,56]

$$SF = \frac{d_{max} - d_{min}}{d_{max} + d_{min}} \quad (8)$$

where d_{max} and d_{min} are the maximum and the minimum diameter of Feret, respectively. This factor varies from zero, for a perfect sphere, up to unity for an elongated particle.

The aspect ratio (AR) gives a good description of large bead deformations but is less accurate on smaller ones. AR varies from unity for a sphere to infinity for an elongated particle and was determined using the following equation:

$$AR = \frac{d_{max}}{d_{min}} \quad (9)$$

where d_{max} and d_{min} have been previously described.[55,56]

The surface morphology and the internal structure of the hydrate systems was investigated using a scanning electron microscope (SEM) equipped with a Peltier cooling-device MK3 Cool stage Carl Zeiss SUPRA with a working distance of about 8 mm and high voltage of 10 KV. Analyses were done around 0 °C in variable pressure mode (20 Pa) using a BSE detector (Signal A BSD4).

3. Results and discussion

3.1 Immobilization of CRL onto Ca-alginate beads

Different experimental conditions were tested to optimize the best composition to obtain stable Ca-alginate beads. Both their size and shape have a noticeable effect on their chemical and mechanical stability, and the production of monodisperse and spherical beads is preferable. The main factors affecting the size and shape of Ca-alginate beads have been previously reported and reviewed.[55,56] Being alginate a family of linear binary copolymers of mannuronic (*M*) and guluronic (*G*) acids, the chemical properties of the commercial alginate used to prepare the beads, namely the molecular weight (MW = 37.6 ± 0.2 kDa) and the composition (M/G = 1.77), influenced their cross-link ability; the data of alginate characterization are reported in ESI† (Tables S1, S2 and Fig. S1). Increasing sodium alginate concentrations were tested to obtain spheres with good mechanical strength, but below 5% (w/v) beads were fragile and broke rapidly under mild magnetic stirring. Among the other parameters that affect the size and shape of the beads, the concentration of calcium chloride in gelation solution and the hardening time in the reticulation bath play an important role. The beads were prepared by extrusion dripping, one of the most popular methods, in which an alginate solution containing the enzyme is extruded through a capillary and dropped into a calcium chloride solution at room temperature. Briefly, CRL was dispersed in the aqueous alginate solution, added dropwise in two different calcium chloride solutions, *i.e.*, 2 and 5% (w/v) and maintained under magnetic stirring at 50 rpm for 10, 30 or 60 min, to obtain six different formulations indicated as **Beads 1–6**, as reported in Table 1.

Fig. 1 shows a schematic representation of the synthetic process for preparing the immobilized CRL on Ca-alginate beads.

3.2 Immobilization efficiency

The amount of the enzyme in the alginate beads, its loss in the preparation procedure and over time were evaluated using the Bradford method for all six different types of beads. In the preparation and washing solutions, the amount of CRL was found to be below the detection limit of the method (22 μg ml^{-1}). Furthermore, to evaluate the effective amount of immobilized enzyme, the catalytic activity of the preparation

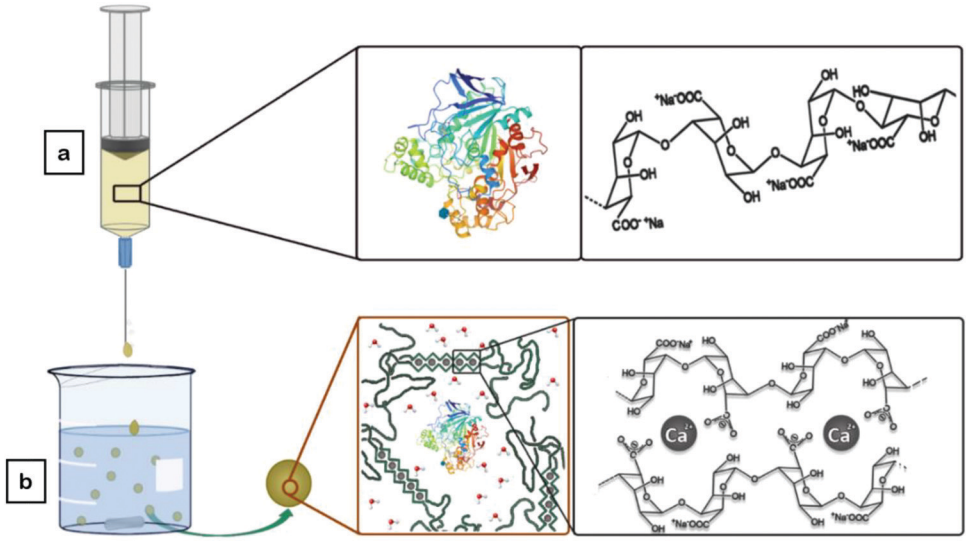

Fig. 1 Schematic representation showing the preparation of CRL encapsulated in Ca-alginate beads: (a) a solution of 5% (w/v) alginate containing CRL (2 mg ml^{-1}) is dropped into a (b) 2 or 5% $CaCl_2$ solution with a residence time of 10, 30 or 60 min.

solution was measured, and the immobilization yield, obtained from eqn (1), resulted of about 94.4%. The immobilization efficiency was also determined as previously described in eqn (2) and turns out to be 76%. These parameters indicated that 18% of the immobilized activity was lost due to entrapment procedure because the enzyme was inactivated or inaccessible to the substrate. As regards the enzyme loss over time, withdrawals of the storage water were taken at different times for one month and subjected to the Bradford assay. The only preparations that had a detectable enzyme loss after 48 h of storage in the aqueous solution, which remained fairly constant over time, were **Beads 1** (1%) and **Beads 2** (0.6%), *i.e.*, those with a shorter residence time in the calcium chloride solution (10 min) (Table S3, ESI†). In the other cases, there was an oscillation of the absorbance values that were below the sensitivity of the detection method.

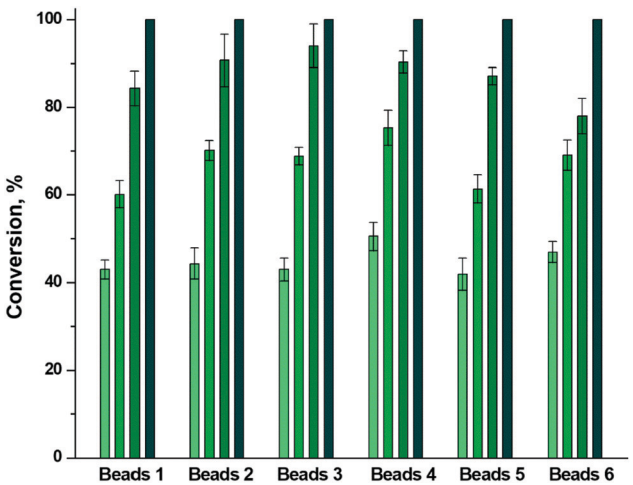

Fig. 2 Substrate conversion percentages for all types of beads at 30 min (■), 1 h (■), 2 h (■) and 3 h (■); [*p*-NPA] = 10 mM, T = 25 °C.

3.3 Hydrolytic activity of enzymatic Ca-alginate beads

Before evaluating the hydrolytic activity of the lipase from *Candida rugosa* in alginate beads, blank tests were performed to rule out that enzyme-free beads catalyze the *p*-NPA hydrolysis reaction.

Once this was established, activity tests were performed with the CRL-containing beads in pure water, rather than in buffer solution. Indeed, notwithstanding the pH of the medium is a critical parameter in enzymatic reactions, since it affects ionization state of enzyme leading to changes in the active site,[57] the presence of salts in the reactor vessel could lead to corrosion issues in view of industrial applications, as biofuel production.[58]

The first catalytic tests were performed with all the bead formulations with *p*-NPA at a concentration of 10 mM. Fig. 2 shows the conversion percentage of the substrate over time for the six types of beads.

The figure clearly shows that, regardless of the bead formulation, all reactions were complete within three hours with an initial reaction rate of 130 ± 10 μM min^{-1}, and only slight differences were observed during the reaction between the different types of beads. Therefore, it was not possible to discriminate them in terms of conversion efficiency if used immediately after their preparation.

In Section 3.2, we proved that there was no leakage of enzyme from the beads during long-term storage, except for **Beads 1** and **Beads 2**, where the loss was still less than or equal to 1%, but we had no information regarding its activity after a long period of storage in water. Therefore, a reaction cycle was performed one month after preparation to evaluate whether the enzyme in the beads was still active. For all types of beads, complete substrate conversion was achieved within four hours

indicating that there were no significant changes in the activity of CRL after a month of storage (Fig. S2, ESI†).

3.4 CRL recyclability

One of the most useful advantages of enzyme immobilization is its reusability, which is of great importance in the production of biocatalysts. For this reason, many papers in the literature deal with the stability and recyclability of CRL immobilized on solid supports by adsorption,[25,27,29] cross-linking,[30] covalent binding,[33–35] or entrapment.[36,38,47,50] Although in most of them the enzyme showed significant stabilization and recyclability, the deactivation of proteins can frequently occur. This effect is often due to the leakage of enzyme from the support or to its conformational limitation; furthermore, low substrate diffusion can also contribute to the loss of catalytic activity.

To assess the reusability of CRL within Ca-alginate beads, the two extreme formulations, **Beads 1** and **Beads 6**, were chosen to perform ten catalytic cycles, in order to evaluate the influence of both $CaCl_2$ concentration and residence time in the solution itself. These tests were carried out with 10 mM substrate and reactions were followed until to completion. Fig. 3 shows the results of repeated uses obtained after 3 h of reaction, which is the time required to the biocatalyst to complete the first cycle.

The data obtained clearly indicated that **Beads 1** and **Beads 6** were able to convert all the substrate into product for the first four and three cycles respectively and, at the tenth cycle, for both formulations the loss of activity was less than 20%. Despite this slightly decrease of relative activity, the reaction time from 3 h to the first cycle increases up to 7 h to the tenth one to reach the complete hydrolysis of the substrate, due to a halving of initial reaction rate for both formulations (from about 120 μM min^{-1} to 60 μM min^{-1}). The results obtained so far showed that there were no differences in terms of catalytic efficiency and recyclability between the different formulations.

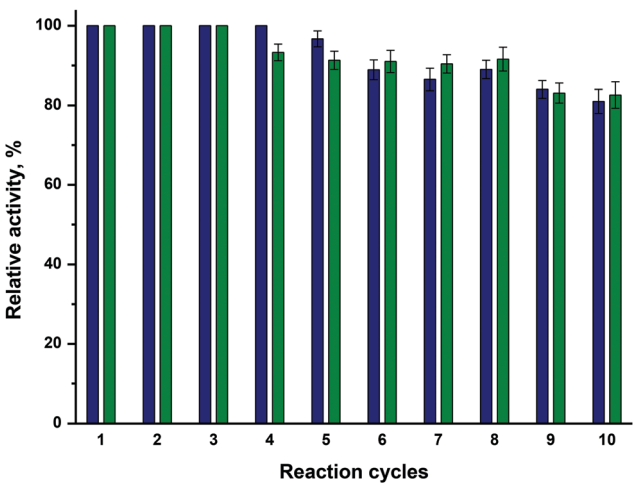

Fig. 3 Residual activity of immobilized CRL in Ca-alginate beads in water after 3 h of reaction: **Beads 1** (■) and **Beads 6** (■); [*p*NPA] = 10 mM, T = 25 °C.

The use of alginate beads in the immobilization of CRL according to our formulations, compared to other systems, shows numerous advantages, as can be seen from Table 2. The preparation of the support is simple and requires only two steps, and high immobilization efficiency, recyclability and storage stability are achieved. Furthermore, our biocatalyst is active in distilled water, avoiding the buffer which is probably the cause of the observed enzyme leakage[46,47] and induces swelling of the beads increasing their fragility (data not shown).

3.5 Morphological studies

The morphological characterization was performed to determine the macro- and microstructure of beads prepared with different concentrations of calcium chloride and residence times in the hardening solution; also in this case, **Beads 1** and **Beads 6** were chosen.

Analyses were initially performed using the stereomicroscope and the results are shown in Fig. 4.

Both **Beads 1** and **Beads 6** showed fairly uniform dimensions and the size distribution of 25 beads was measured, since the variance coefficient (CV), determined using eqn (7), was 0.9 and 3.7% respectively. Table 3 reports some of the dimensionless shape indicators quantified using eqn (8) and (9) (Section 2.8).

Both bead formulations have similar dimensions of about 3 mm, but better spherical shape was obtained with **Beads 1**, which are those prepared with lower calcium chloride concentration and shorter hardening time, since SF $<$ 0.05 and AR was slightly higher than unity.[56] On the other hand, **Beads 6**, as already visible from the stereomicroscope image, are less spherical; their SF value was very similar to that of alginate particles reported in the literature and prepared with our same experimental conditions, *i.e.* concentration of alginate and $CaCl_2$, and hardening time.[66] Then, the analyses by the scanning electron microscope were performed on both the external surface and the internal structure (by cutting them with a scalpel). Generally, in literature, SEM morphological studies are conducted on dehydrated beads, providing information that often does not correspond to the real systems employed in catalytic tests, which are hydrated. To avoid dehydration of the samples, the application of variable-pressure equipment (VP-SEM) and Peltier cooling-device allows the investigation of wet samples and hydrated systems in SEM.[67] Thanks to the aid of this methodology, in this study we were able to investigate the samples in their operating conditions. The SEM images were acquired at different magnifications and the most significant at 70x and 300x are shown in Fig. 5.

Although no significant differences were detected from their external surface, the analysis of the cross section highlighted less internal compactness of **Beads 1** than that of **Beads 6** which seemed denser and more homogeneous. Further SEM analyses were then performed to understand if the cause of this different internal morphology was due to the $CaCl_2$ concentration and/or to the hardening time. For these analyses, **Beads 2** ($CaCl_2$ 5%, 10 min) and **Beads 5** ($CaCl_2$ 2%, 60 min) were selected and SEM images, reported in Fig. S3 (ESI†) of both the whole beads and the internal structure highlighted that the

Table 2 Comparison of our immobilization system with those of the literature in terms of preparation, yield of immobilization, recycling, and storage

Immobilization method	Preparation step	Biocatalyst	Immobilization yield	Substrate	Recycle times	Residual activity	Operational condition	Storage stability (days)	Residual activity	Ref.
Covalent immobilization onto a solid carrier (MOF)	2	*Candida rugosa* lipase (CRL) type VII	CRL-ZIF-8 8.18%, mCRL-ZIF-8 9.45%	*p*-Nitrophenyl palmitate	7	CRL-ZIF-8 45.8%, mCRL-ZIF-8 52.3%	Isopropanol- PBS pH 7,5 (1 : 9) 35 °C	7	CRL-ZIF-8 34.42%, mCRL-ZIF-8 42.18%	32
Covalent immobilization onto a ternary support (CRL-ALG/NC/MMT)	5	*Candida rugosa* lipase (CRL) type VII	2.9%	Levulinic acid	9	47.5%	Ethanol 50 °C	—	—	34
Covalent immobilization on magnetic beads	5	*Candida rugosa* lipase (CRL)	—	Racemic ibuprofen	5	100%	Cyclohexane 37 °C	—	—	35
Sol–gel encapsulation in presence of magnetic sporopollenin/Fe_3O_4 nanoparticles	4	*Candida rugosa* lipase (CRL)	Fe-A-Spo-E 36%, Fe-EP-Spo-E 89%	*p*-Nitrophenyl palmitate	7	Fe-A-Spo-E 21%, Fe-EP-Spo-E 63%	Isopropanol – PBS pH 7 37 °C	50	Fe-A-Spo-E 45%, Fe-EP-Spo-E 40%	36
Sol–gel encapsulation e with Fe_3O_4 or Fe_3O_4-Spo	5	*Candida rugosa* lipase (CRL) type VII	Fe_3O_4 78.6%, Fe_3O_4-Spo 76.2%	Racemic naproxen methyl ester	5	Fe_3O_4-E 36%, Fe_3O_4-Spo 64%	Aqueous phase–organic solvent (PBS pH 7 – isooctane)	42	Fe_3O_4 >70%, Fe_3O_4-Spo >90%	37
Sol–gel encapsulation with *b*-cyclodextrin grafted magnetic nanoparticles (CD-APS-NP)	5	*Candida rugosa* lipase (CRL) type VII	2.2%	*p*-Nitrophenyl palmitate	6	~50%	PBS buffer (pH 7.0) 35 °C	—	—	38
Sol–gel Encapsulation in the presence of magnetic calix[4]arene nanoparticles	4	*Candida rugosa* lipase (CRL)	3.2%	Racemic naproxen methyl ester	5	28%	Aqueous phase–organic solvent (PBS – isooctane)	—	—	39
Covalent immobilization on magnetite coated with nanosilica	5	*Candida rugosa* lipase (CRL)	~80%	*n*-Butyric acid and 1-butanol (1 : 2)	17	50%	*n*-Heptane at 45 °C	—	—	59
Encapsulation in chitosan nanoparticles	3	*Candida rugosa* lipase (CRL)	—	Olive oil	7	53%	Water–oil (1 : 1) 37 °C	—	—	60
Entrapment in Ca-alginate beads	2	*Candida rugosa* lipase (CRL)	35%	*p*-Nitrophenyl butyrate	3	72%	Tris–HCl buffer (pH 7.2); 30 °C	—	—	47
Covalent immobilization of lipase onto the silica nanoflowers-NH2	3	*Candida antarctica* lipase	~57%	Levulinic acid and ethanol (1 : 10)	8	68%	*Tert*-butyl methyl ether 40 °C	—	—	61
Freeze dried calcium alginate beads	3	*Candida antarctica* lipase B (CALB)	—	*p*-Nitrophenyl butyrate	6	~90%	Distilled water 35 °C	16	~100%	62
Immobilization on magnetic sol–gel hybrid organic-inorganic (Fe_3O_4 MNPs@TEOS-TSD@CALB)	4	*Candida antarctica* lipase B (CALB)	90%	Waste cooking oil	10	16.5%	Methanol; 40 °C	—	—	63
Covalent immobilization on polydopamine functionalized magnetic mesoporous biochar (MPCB-DA)	6	*Bacillus licheniformis* lipase	46.5%	*p*-Nitrophenyl palmitate	10	56%	Tris–HCl (50 mM, pH 8.5); 40 °C	70	88% at 25 °C	64
Covalent immobilization on hydroxyapatite/glycyrrhizin/lithium-based metal–organic framework (HA/GL/Li-MOF) nanocomposites	5	*Thermomyces lanuginosus* lipase (TLL)	TLL@HA/GL/Li-MOF 71%, TLL@Li-MOF 68%	*p*-Nitrophenyl palmitate	10	TLL@HA/GL/Li-MOF ~55%, TLL@Li-MOF ~45%	Carbonate bufer (100 mM, pH 9.0); 60 °C	30	TLL@HA/GL/Li-MOF ~30%, TLL@Li-MOF ~20%	65
Entrapment inside Ca-Alginate beads	2	*Candida rugosa* lipase (CRL) type VII	94.4%	*p*-Nitrophenyl acetate	10	>80%	Distilled water 25 °C	30	~100%	Current work

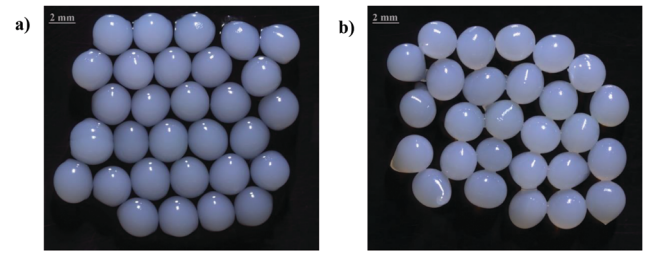

Fig. 4 Stereomicroscope images at 1*x* magnification of **Beads 1** (a) and **Beads 6** (b).

Table 3 Average diameters of **Beads 1** and **Beads 6** and their sphericity indicators

	Beads 1	Beads 6
Average diameter (D_m)	3.2 mm	3.4 mm
Sphericity factor (SF)	0.031	0.069
Aspect ratio (AR)	1.06	1.15

internal compactness depends on the gelation time and not on $CaCl_2$ concentration.

3.6 Reaction with *p*-nitrophenyl dodecanoate

The *p*-nitrophenyl dodecanoate (*p*-NPD) was then chosen to evaluate the efficiency of CRL immobilized on **Beads 1** and **6** on a more hydrophobic substrate. Being poorly soluble in water, *p*-NPD hydrolysis reaction was carried out in a sterically hindered alcohol, *i.e.*, *tert*-butyl alcohol, in order to avoid or at least reduce the competitive transesterification reaction rate. In this case, the conversion efficiency of the two formulations was very different. In fact, **Beads 1** were able to completely hydrolyze the substrate in 6 h, while the rate of the reaction catalyzed by **Beads 6** was very low: after 6 h, little more than 40% of product was formed and increased slowly over time (Fig. S4, ESI†). The reaction did not complete even after 24 h, being the conversion equal to 80%. This result clearly indicated that the internal structure of **Beads 6** compared to **Beads 1** limited the mass transfer of reagents and/or products in the reaction medium and this drawback was evident with large, hydrophobic substrates and therefore much more similar to natural ones. On the other hand, **Beads 1**, thanks to their lower compactness, were able to ensure the free diffusion of reagents within their porous structure.

Furthermore, the time taken by **Beads 1** to completely hydrolyze *p*-NPD was twice than that required for the reaction with *p*-NPA. Therefore, to determine if the increase in reaction time was due to the substrate or to the solvent, the reaction of *p*-NPA in *tert*-butyl alcohol was performed for comparison purpose (Fig. S5, ESI†). After 48 h, only 58% of conversion was achieved, and this result can be explained by the dehydration of the beads that became smaller and smaller over time. The loss of water from the confined environment in which the enzyme is located led to the observed slowdown of the reaction. This hypothesis was confirmed by experiments performed by

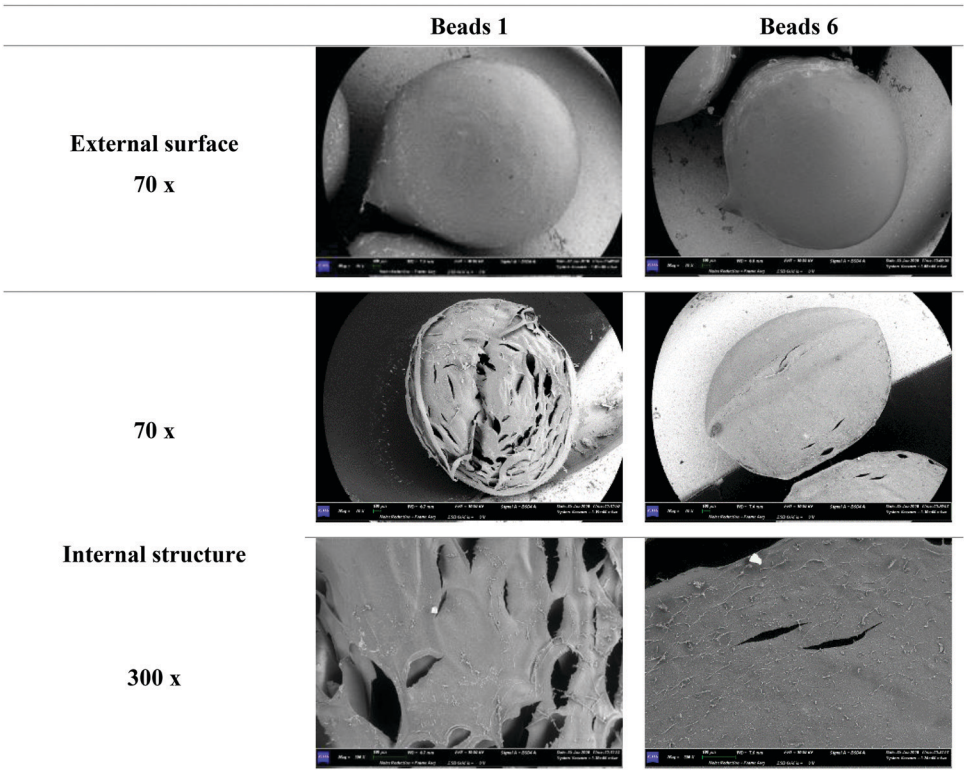

Fig. 5 SEM images at 70*x* magnification of the external structure and at 70*x* and 300*x* magnifications of the internal structure of **Beads 1** and **Beads 6**.

varying the amount of water inside the reaction medium; the time required for complete hydrolysis of the *p*-NPA was decreased from 24 to 4 h with a water percentage of 5% and 75% respectively (Fig. S6, ESI†).

Therefore, given all the considerations made so far, the **Beads 1** formulation, being one of the fastest preparations and ensuring better mass transfer, thus allowing their possible use with a wide range of substrates, has been chosen to perform thermostability tests and kinetic resolution of (*R*,*S*)-1-phenylethyl acetate.

3.7 Thermostability

One of the advantages of enzyme immobilization is the improvement of thermal stability. Therefore, the stability of both free and immobilized lipase in **Beads 1** were determined by incubating them for different times and the residual activity was measured at 25.0 ± 0.1 and 50.0 ± 0.1 °C (Fig. 6).

The effect of immobilization on Ca-alginate beads on CRL stability is clearly highlighted by the figure at both investigated temperatures. Immobilized CRL activity at 25 °C did not decrease after 7 days of incubation while the free form lost 30% of its initial activity after 5 days and 60% after one week. Even more evident was the stabilization effect at 50 °C. In fact, the residual activity of free lipase, after only 8 h, was lower than 40% and continued to decrease over time until reaching a value of about 20% after one week of incubation. On the other hand, the remaining activity of immobilized CRL was about 70% after 1 day of heat treatment and remained unchanged throughout the week.

Moreover, stability tests were carried out with **Beads 6** at 50 °C to assess the effect of their higher compactness on the enzyme thermal stability. They showed that the different operational conditions used in the preparation of the two formulations did not affect the stability of the enzyme, being the loss of activity after 24 h equal to 66% (data not shown).

The data reported in Fig. 6 show the trends of residual activity over time, but do not consider the differences in the reaction rate before incubation. In particular, hydrolysis rate with free CRL was 30% higher than that of immobilized one both at 25 °C (183 *vs.* 132 μM min^{-1}) and 50 °C (520 *vs.* 370 μM min^{-1}). This effect could be due to a slower diffusion of the substrate inside the support. However, after a week of incubation the reaction rate of **Beads 1** at 25 °C and 50 °C was 2 times higher than that of the free enzyme, thanks to the improvement in enzymatic stabilization following the entrapment.

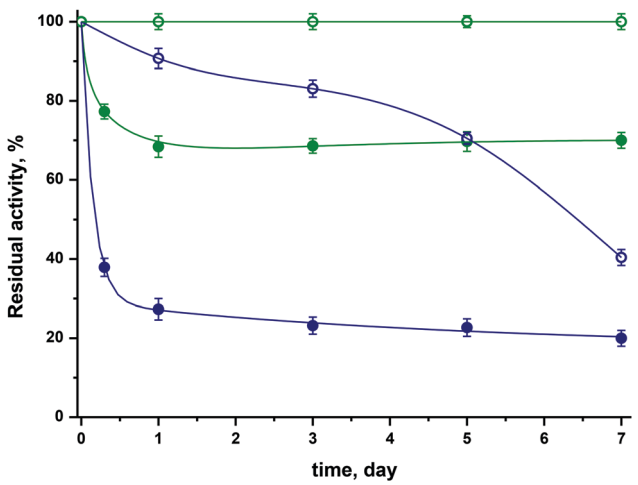

Fig. 6 Thermal stability of free (●/○) and immobilized lipase (●/○) at 25 °C (empty symbols) and 50 °C (closed symbols).

3.8 Kinetic resolution of (*R*,*S*)-1-phenylethyl acetate

Many studies have been devoted to the kinetic resolution of racemic substrates with pharmacological activity, such as naproxen[30,37,68] and ibuprofen[35] by using immobilized CRL, since the enantiomers of these non-steroidal anti-inflammatory drugs demonstrate different therapeutic activities.

Given the excellent recyclability and thermal stability of **Beads 1**, and therefore their possible application in industrial processes, they were used in preliminary tests for the resolution of (*R*)-1-phenylethanol in aqueous solution starting from racemic 1-phenylethyl acetate as model substrate. In the literature, several papers report about the stereoselective kinetic resolution of *rac*-1-phenylethyl acetate catalyzed by other lipases,[69–73] in which very high enantiomeric excess towards the (*R*)-enantiomer were obtained, but with not too satisfying yields. More recently, marine microbial GDSL lipase MT6 showed opposite stereoselectivity, as it hydrolyzed racemic 1-phenylethyl acetate to generate (*S*)-1-phenylethanol instead of (*R*)-1-phenylethanol.[74] During reaction course, as the conversion increased, the *ee* of the product (ee_p) decreased and, at the optimal reaction time (12 h), a conversion of 28.5% with an *ee* value of the substrate (ee_s) higher than 97% was obtained. On the other hand, CRL solubilized in phosphate buffer at pH 7.2 showed no enantiopreference for the (*R*)-acetate with an *ee* value of only 44% and an enantioselectivity factor of 4.[75]

Here, the course and selectivity of the kinetic resolution of (*R*,*S*)-1-phenylethyl acetate were checked, as reported in materials and methods, by chiral HPLC and all the chromatograms are shown in Fig. S7 (ESI†). The percentage of enantiomeric excess (ee_s and ee_p), conversion (*c*) as well as enantioselectivity (*E*), determined using eqn (3)–(6), are reported in Table 4.

As observed from these results, while ee_s increased with reaction time and conversion, ee_p remained almost constant. After 96 h of reaction, the highest values of enantioselectivity (*E* = 10.3), conversion (*c* = 57.8%) and enantiomeric excess of substrate (ee_s = 83.3%) were observed. These values are slightly

Table 4 Enantiomeric excess of both substrate (ee_s) and product (ee_p), conversion (*c*) and enantioselectivity (*E*) of the hydrolysis reaction of (*R*,*S*)-1-phenylethyl acetate using **Beads 1** at 25 °C

Reaction time (h)	ee_s, %	ee_p, %	*c*, %	*E*
8	3.5	61.5	5.3	4.3
24	17.6	62.8	21.9	5.2
32	18.1	61.9	22.6	5.1
48	23.1	64.5	26.4	5.8
72	49.5	61.7	44.5	6.8
96	83.3	60.9	57.8	10.3

higher but do not differ so much from those reported in the literature regarding free lipase in phosphate buffer, which showed an ee_s value of 44% and an enantioselectivity factor of 4.[75] Given the intrinsic chirality of the matrix, we performed these tests to assess whether the immobilization improved the enantioselectivity of the enzyme towards the chosen substrate. This has not happened, but the entrapment of CRL improved its stability under non-physiological conditions and temperatures and made it recyclable for multiple cycles, which is essential for industrial applications.

4. Conclusion

In this study, lipase from *Candida rugosa* was efficiently trapped in Ca-alginate beads prepared using different operating conditions. Morphological studies highlighted that, despite differing in their internal microstructure, all formulations exhibited high immobilization efficiency, good recyclability and stability, both operational and thermal. The effectiveness of the immobilized CRL was instead dependent on the hydrophobicity of the substrate. The higher internal compactness of **Beads 6**, compared to **Beads 1**, did not affect the hydrolysis rate of *p*-NPA, but limited the mass transfer of the more hydrophobic substrate *p*-NPD causing a notable decrease in its reaction rate. Further studies will be performed to improve the stereoselectivity of the immobilized biocatalyst by modifying either the operational conditions or the bead composition.

Author contributions

A. Vetrano: investigation, validation, writing-original draft; F. Gabriele: investigation, visualization, writing-review & editing; R. Germani: conceptualization, writing-review & editing; N. Spreti: conceptualization, writing-review & editing, supervision.

Conflicts of interest

There are no conflicts to declare.

Acknowledgements

We would like to acknowledge financial support from the Ministero dell'Università e della Ricerca, MIUR (Rome, Italy). The Authors thank Dr Lorenzo Arrizza (Microscopy Centre, University of L'Aquila) for his kindly assistance in SEM analysis.

References

1 R. A. Sheldon and J. M. Woodley, *Chem. Rev.*, 2018, **118**, 801–838.
2 R. A. Sheldon and S. van Pelt, *Chem. Soc. Rev.*, 2013, **42**, 6223–6235.
3 R. C. Rodrigues, C. Ortiz, Á. Berenguer-Murcia, R. Torres and R. Fernández-Lafuente, *Chem. Soc. Rev.*, 2013, **42**, 6290–6307.
4 R. C. Rodrigues, J. J. Virgen-Ortíz, J. C.-S. dos Santos, Á. Berenguer-Murcia, A. R. Alcantara, O. Barbosa, C. Ortiz and R. Fernandez-Lafuente, *Biotechnol. Adv.*, 2019, **37**, 746–770.
5 R. C. Rodrigues, Á. Berenguer-Murcia, D. Carballares, R. Morellon-Sterling and R. Fernandez-Lafuente, *Biotechnol. Adv.*, 2021, **52**, 107821.
6 J. Zdarta, A. S. Meyer, T. Jesionowski and M. Pinelo, *Catalysts*, 2018, **8**, 92.
7 J. C.-S. D. Santos, O. Barbosa, C. Ortiz, A. Berenguer-Murcia, R. C. Rodrigues and R. Fernandez-Lafuente, *ChemCatChem*, 2015, **7**, 2413–2432.
8 S. Cantone, V. Ferrario, L. Corici, C. Ebert, D. Fattor, P. Spizzo and L. Gardossi, *Chem. Soc. Rev.*, 2013, **42**, 6262–6276.
9 R. A. Sheldon, *Adv. Synth. Catal.*, 2007, **349**, 1289–1307.
10 S. García-Embid, F. Di Renzo, L. De Matteis, N. Spreti and J. M. de la Fuente, *Appl. Catal., A*, 2018, **560**, 94–102.
11 L. De Matteis, R. Germani, M. V. Mancini, F. Di Renzo and N. Spreti, *Appl. Catal. A Gen.*, 2015, **492**, 23–30.
12 L. De Matteis, R. Germani, M. V. Mancini, G. Savelli, N. Spreti, L. Brinchi and G. Pastori, *J. Mol. Catal. B: Enzym.*, 2013, **97**, 23–30.
13 C. Garcia-Galan, Á. Berenguer-Murcia, R. Fernandez-Lafuente and R. C. Rodrigues, *Adv. Synth. Catal.*, 2011, **353**, 2885–2904.
14 B. P. Dwivedee, S. Soni, M. Sharma, J. Bhaumik, J. K. Laha and U. C. Banerjee, *ChemistrySelect*, 2018, **3**, 2441–2466.
15 P. Choudhury and B. Bhunia, *Biopharm J.*, 2015, **1**, 41–47.
16 B. Andualema and A. Gessesse, *Biotechnology*, 2012, **11**, 100–118.
17 F. Hasan, A. A. Shah and A. Hameed, *Enzyme Microb. Technol.*, 2006, **39**, 235–251.
18 A. Houde, A. Kademi and D. Leblanc, *Appl. Biochem. Biotechnol.*, 2004, **118**, 155–170.
19 R. D. Schmid and R. Verger, *Angew. Chem., Int. Ed.*, 1998, **37**, 1608–1633.
20 J. Barriuso, M. E. Vaquero, A. Prieto and M. J. Martínez, *Biotechnol. Adv.*, 2016, **34**, 874–885.
21 P. Domínguez De María, J. M. Sánchez-Montero, J. V. Sinisterra and A. R. Alcántara, *Biotechnol. Adv.*, 2006, **24**, 180–196.
22 S. Benjamin and A. Pandey, *Yeast*, 1998, **14**, 1069–1087.
23 E. Subroto, R. Indiarto, A. D. Pangawikan, S. Huda and V. P. Yarlina, *Food Res.*, 2020, **4**, 1391–1401.
24 M. Matsumoto and K. Ohashi, *Biochem. Eng. J.*, 2003, **14**, 75–77.
25 H. Aghaei, M. Ghavi, G. Hashemkhani and M. Keshavarz, *Int. J. Biol. Macromol.*, 2020, **162**, 74–83.
26 R. D.-M. Ferreira, R. Brackmann, E. B. Pereira and R. D.-C. da Rocha, *Appl. Biochem. Biotechnol.*, 2020, **190**, 839–850.
27 L. T. Izrael Živković, L. S. Živković, V. P. Beškoski, K. R. Gopčević, B. M. Jokić, D. S. Radosavljević and I. M. Karadžić, *J. Mol. Catal. B: Enzym.*, 2016, **133**, S533–S542.
28 L. Izrael-Zivkovic, L. Zivkovic, B. Jokic, A. Savic and I. Karadzic, *J. Serb. Chem. Soc.*, 2015, **80**, 1113–1125.

29 L. T. Izrael Živković, L. S. Živković, B. M. Babić, M. J. Kokunešoski, B. M. Jokić and I. M. Karadžić, *Biochem. Eng. J.*, 2015, **93**, 73–83.
30 S. Salgın, M. Çakal and U. Salgın, *Prep. Biochem. Biotechnol.*, 2020, **50**, 148–155.
31 S. Velasco-Lozano, F. López-Gallego, J. Rocha-Martin, J. M. Guisán and E. Favela-Torres, *J. Mol. Catal. B: Enzym.*, 2016, **130**, 32–39.
32 J. C. Wu, V. Selvam, H. H. Teo, Y. Chow, M. M.-R. Talukder and W. J. Choi, *Biocatal. Biotransform.*, 2006, **24**, 352–357.
33 B. Zou, L. Zhang, J. Xia, P. Wang, Y. Yan, X. Wang and I. O. Adesanya, *Appl. Biochem. Biotechnol.*, 2020, **192**, 132–145.
34 F. N.-N. Mohd Hussin, N. Attan and R. A. Wahab, *Enzyme Microb. Technol.*, 2020, **136**, 109506.
35 M. P. Marszałł and T. Siódmiak, *Catal. Commun.*, 2012, **24**, 80–84.
36 E. Ozyilmaz, K. Etci and M. Sezgin, *Prep. Biochem. Biotechnol.*, 2018, **48**, 887–897.
37 E. Yilmaz, M. Sezgin and M. Yilmaz, *J. Mol. Catal. B: Enzym.*, 2011, **69**, 35–41.
38 E. Ozyilmaz, S. Sayin, M. Arslan and M. Yilmaz, *Colloids Surf., B*, 2014, **113**, 182–189.
39 S. Sayin, E. Yilmaz and M. Yilmaz, *Org. Biomol. Chem.*, 2011, **9**, 4021–4024.
40 W. Xie and X. Zang, *Food Chem.*, 2018, **257**, 15–22.
41 W. Xie and X. Zang, *Food Chem.*, 2017, **227**, 397–403.
42 W. Xie and J. Wang, *Energy Fuels*, 2014, **28**, 2624–2631.
43 W. Xie and M. Huang, *Energy Convers. Manag.*, 2018, **159**, 42–53.
44 M. Bilal and H. M.-N. Iqbal, *Int. J. Biol. Macromol.*, 2019, **130**, 462–482.
45 K. Yong and D. J. Mooney, *Prog. Polym. Sci.*, 2012, **37**, 106–126.
46 S. S. Betigeri and S. H. Neau, *Biomaterials*, 2002, **23**, 3627–3636.
47 K. Won, S. Kim, K. J. Kim, H. W. Park and S. J. Moon, *Process Biochem.*, 2005, **40**, 2149–2154.
48 C. H. Ng and K. L. Yang, *Enzyme Microb. Technol.*, 2016, **82**, 173–179.
49 R. Dave and D. Madamwar, *Process Biochem.*, 2006, **41**, 951–955.
50 C. H. Yang, C. C. Yen, J. J. Jheng, C. Y. Wang, S. S. Chen, P. Y. Huang, K. S. Huang and J. F. Shaw, *Molecules*, 2014, **19**, 11800–11815.
51 M. M. Bradford, *Anal. Biochem.*, 1976, **72**, 248–254.
52 J. Boudrant, J. M. Woodley and R. Fernandez-Lafuente, *Process Biochem.*, 2020, **90**, 66–80.
53 Y. Ji, Z. Wu, P. Zhang, M. Qiao, Y. Hu, B. Shen, B. Li and X. Zhang, *Biochem. Eng. J.*, 2021, **169**, 107962.
54 C. S. Chen, Y. Fujimoto, G. Girdaukas and C. J. Sih, *J. Am. Chem. Soc.*, 1982, **104**, 7294–7299.
55 B. B. Lee, P. Ravindra and E. S. Chan, *Chem. Eng. Technol.*, 2013, **36**, 1627–1642.
56 E. S. Chan, B. B. Lee, P. Ravindra and D. Poncelet, *J. Colloid Interface Sci.*, 2009, **338**, 63–72.
57 Y. Liu, Q. Jin, L. Shan, Y. Liu, W. Shen and X. Wang, *Ultrason. Sonochem.*, 2008, **15**, 402–407.
58 E. Torsner, *Corros. Eng., Sci. Technol.*, 2010, **45**, 42–48.
59 E. Onoja, S. Chandren, F. I.-A. Razak and R. A. Wahab, *J. Biotechnol.*, 2018, **283**, 81–96.
60 M. Weng, C. Xia, S. Xu, Q. Liu, Y. Liu, H. Liu, C. Huo, R. Zhang, C. Zhang and Z. Miao, *Colloid Polym. Sci.*, 2022, **300**, 41–50.
61 B. Jia, C. Liu and X. Qi, *Fuel Process. Technol.*, 2020, **210**, 106578.
62 S. Zhang, W. Shang, X. Yang, S. Zhang, X. Zhang and J. Chen, *Bull. Korean Chem. Soc.*, 2013, **34**, 2741–2746.
63 E. Parandi, M. Safaripour, M. H. Abdellattif, M. Saidi, A. Bozorgian, H. Rashidi Nodeh and S. Rezania, *Fuel*, 2022, **313**, 123057.
64 J. Zhao, M. Ma, X. Yan, G. Zhang, J. Xia, Z. Zeng, P. Yu, Q. Deng and D. Gong, *Food Chem.*, 2022, **379**, 132–148.
65 A. Ameri, F. Asadi, M. Shakibaie, A. Ameri, H. Forootanfar and M. Ranjbar, *Appl. Biochem. Biotechnol.*, 2022, **194**, 2108–2134.
66 A. K. Tamo, I. Doench, A. M. Helguera, D. Hoenders, A. Walther and A. O. Madrazo, *Polymers*, 2020, **12**, 1–24.
67 A. Wassilkowska and T. Woźniakiewicz, *Solid State Phenom.*, 2015, **231**, 139–144.
68 E. Yilmaz, K. Can, M. Sezgin and M. Yilmaz, *Bioresour. Technol.*, 2011, **102**, 499–506.
69 I. Bustos-Jaimes, Y. García-Torres, H. C. Santillán-Uribe and C. Montiel, *J. Mol. Catal. B: Enzym.*, 2013, **89**, 137–141.
70 F. Kartal and A. Kilinc, *Biotechnol. Prog.*, 2012, **28**, 937–945.
71 I. Bustos-Jaimes, W. Hummel, T. Eggert, E. Bogo, M. Puls, A. Weckbecker and K. E. Jaeger, *ChemCatChem*, 2009, **1**, 445–448.
72 Y. Gao, R. Zhong, J. Qin and B. Lin, *Chem. Lett.*, 2009, **38**, 262–263.
73 E. M. Hill, J. M. Broering, J. P. Hallett, A. S. Bommarius, C. L. Liotta and C. A. Eckert, *Green Chem.*, 2007, **9**, 888–893.
74 D. Deng, Y. Zhang, A. Sun and Y. Hu, *Chin. J. Catal.*, 2016, **37**, 1966–1974.
75 F. Bellezza, A. Cipiciani, G. Cruciani and F. Fringuelli, *J. Chem. Soc., Perkin Trans. 1*, 2000, 4439–4444.